Available online at www.sciencedirect.com
ScienceDirect
Journal of Computational Physics 221 (2007) 422–438
JOURNAL OF COMPUTATIONAL PHYSICS
www.elsevier.com/locate/jcp

Finite difference time domain dispersion reduction schemes

Bezalel Finkelstein, Raphael Kastner *

Department of Physical Electronics, School of Electrical Engineering, Tel-Aviv University, Tel-Aviv 69978, Israel

Received 11 October 2005; received in revised form 21 May 2006; accepted 9 June 2006
Available online 24 October 2006

Abstract

The finite-difference-time-domain (FDTD), although recognized as a flexible, robust and simple to implement method for solving complex electromagnetic problems, is subject to numerical dispersion errors. In addition to the traditional ways for reducing dispersion, i.e., increasing sampling rate and using higher order degrees of accuracy, a number of schemes have been proposed recently. In this work, an unified methodology for deriving new difference schemes is presented. It is based on certain modifications of the characteristic equation that accompanies any given discretized version of the wave equation. The method is duly compared with existing schemes and verified numerically.

Keywords: Numerical methods; Finite difference time domain; Numerical dispersion error reduction; Wave equation; Electromagnetics

1. Introduction

The finite-difference-time-domain (FDTD) [1] has long been established as a flexible and robust method that is simple to implement for solving the complex electromagnetic problems. The method has thus become very popular, in particular in its second-order accurate, central differences variant known as the (2,2) scheme. In spite of its advantages, the method is subject to numerical dispersion errors that tend to hinder its application in problems involving narrow pulses and large time spans.

Two traditional ways have been used for the purpose of reducing dispersion, i.e., increasing sampling rate and using higher order degrees of accuracy beyond the classic (2,2) central differencing as used originally by Yee [1]. Higher order explicit approximations for Maxwell's equations, based on Yee's staggered grid, were introduced in [2]. The superior accuracy and efficiency over Yee's scheme was confirmed and quantified in [3,4]. Later, Liu showed [5] that the spatial part of the central difference second-order discrete wave equation can be arrived at either by using Yee's staggered uncolocated scheme or by his newly developed unstaggered scheme, where he used a backward difference on $\nabla \times \mathbf{H}$ and forward difference on $\nabla \times \mathbf{E}$. He then generalized his scheme to a higher order combination of upwind and the corresponding antisymmetric differencing. Further, he derived a fourth-order spatial discretization scheme as a special case with two options of time

* Corresponding author. Tel.: +972 3 6407447; fax: +972 3 6423508.
E-mail address: kast@eng.tau.ac.il (R. Kastner).

0021-9991/$ - see front matter
doi:10.1016/j.jcp.2006.06.016

discretization, i.e., second-order leapfrog and fourth-order Runge–Kutta. Fang's (2,4) algorithm [2] was reformulated in [6] in a compact and simple way, that allowed for the investigation of its dispersion properties and interaction with different boundary conditions. The question of boundary condition for higher order schemes was also addressed in [7]. Other noteworthy contributions on explicit high order FDTD methods are [8], where a variant of Fang's (4,4) scheme was developed based on a variation on the fourth-order time discretization. Implicit compact high order methods for solving Maxwell's equations can be found in [9–13]. Alternative methods for accuracy enhancement may be categorized in belonging to one of three groups. The first and most widely used group has its roots in the early work by Miranker [14]. Realizing that the truncated Taylor series may not be the most accurate way to discretize the wave equation, he suggested a minimization of a functional containing Fourier components of the solution. Miranker produced explicit time marching schemes by analytically solving constrained minimization problems with quadratic cost. Due to the complexity of the analytic calculation required, Miranker's method went relatively unnoticed until rediscovered in the early 90's by Lele [15], who constructed a class of highly accurate compact schemes for first, second and higher derivatives. Lele attained high accuracy by using a 7-point stencil, although without exploiting its full capacity in order to get high order Taylor series accuracy; rather, he used a portion of the series to make the discrete operator equal to the continuous one at three predefined high frequencies. Tam and Webb [16] devised an explicit high order spatial and temporal algorithm for solving the linearized Euler equation encountered in acoustics. They referred their scheme as a Dispersive Relation Preserving one (DRP). Haras and Ta'asan [17] used Miranker's minimization approach combined with Lele's implicit compact discretization to create their version of a high order scheme. Liu [5] used a discretized first derivative operator (upwind) and its antisymmetric one to create a nonstaggered scheme to solve Maxwell's equation. The coefficients in this scheme are determined by solving a Miranker-type functional numerically. Recently, Wang and Teixeira published a series of papers [18–21] employing artificial dispersion and adjustable coefficients with high frequency digital filtering to create optimized DRP schemes. Zygiridis and Tsiboukis [22] and Sun and Trueman [23] devised an optimized scheme based on a staggered (2,4) stencil. Another recent work in this context is [24].

The second group is based on Mickens's nonstandard FDTD (NSFDTD) method [25]. In this method, one creates difference schemes with solutions that are exact replicas of the solutions to their continuous PDE counterparts, using a generalization of the traditional approximation to the derivative operator. As opposed to the complex minimization processes required to construct the difference schemes of the first group, Mickens's scheme finds a suitable function to generalize the derivatives of a specific PDE thus expressing the difference scheme coefficients in an explicit manner. This method was applied to CEM in [26], where the wave equation was dicretized by using a linear combination of conventional in addition to diagonal discretizing (2,2) schemes in order to improve isotropy properties at a single predefined frequency. This scheme was later modified [27] to accommodate Yee's staggered grid, and to improve stability and provide time step analysis [28]. In [29], Mickens's strategy was utilized to better discretize 1D, 2D and 3D Helmholtz equations and the temporal Maxwell's equations. Recently, Yang and Balanis have devised in [30,31] an improved nonstandard finite difference to mitigate anisotropy in (2,2) and (2,4), respectively, Yee type stencils.

Finally, the third group includes [32] where Maxwell's equations are used in their integral form to produce a modified (2,4) explicit algorithm with two adjustable parameters to minimize phase error. In [33,34], Yee's and Bi's [35] types of grids, having complementary phase behavior are combined to produce an almost isotropic scheme. Finally, a moment-like expansion of the fields has been employed to produce more accurate solutions. The use of scaling and wavelet functions in approximations for the spatial derivative operator was shown in [36], and a recent flexible local approximation method (FLAME) [37] makes use of functions that are solutions to Maxwell's equations as a basis to expand the field components in both time and space.

In this work, we develop an unified methodology for deriving new difference schemes that can accommodate arbitrary requirements for reduced phase or group velocity dispersion errors, defined over any region in the frequency-direction space. The preferred starting point for this development is an unified formulation for all schemes involving the characteristic equation, as outlined in Section 2. A general strategy for developing various dispersion reduction schemes is based on certain systematic modifications of the characteristic equations, as presented in Section 3. This strategy is then spelled out for cases such as several 1D wave equation FDTD schemes (Section 4) and the 2D (2,2) FDTD scheme (Section 5). Analytical comparison with other schemes is done in Section 6. Analysis of dispersion curves is carried out in Section 7, where regions of better

performance can be seen and explained, and numerical examples of a propagating pulse verify the effects in Section 8. Finally, conclusions are drawn in Section 9.

2. Dispersion relationships and stability criteria revisited via an unified formulation of the characteristic equation

2.1. Definitions of characteristic equations

A convenient starting point for the analysis and synthesis of both dispersion and stability is the characteristic equation (CE) that distills the properties of the difference equations, as in the following conventional cases.

2.1.1. The one-dimensional wave equation

The continuous wave equation

$$\left(\frac{\partial^2}{\partial x^2}-\frac{1}{c^2}\frac{\partial^2}{\partial t^2}\right)u(x,t)=0 \tag{1}$$

is customarily discretized via the second-order accurate, central difference scheme, leading to the following (2,2) difference equation:

$$u_i^{n+1}-2u_i^n+u_i^{n-1}-\gamma^2\left(u_{i+1}^n-2u_i^n+u_{i-1}^n\right)=0 \tag{2}$$

with $x=\mathrm{i}\Delta x$, $t=n\Delta t$ and $\gamma=c\frac{\Delta t}{\Delta x}$ (the Courant number). Invoking separation of variables, using power-type eigenfunctions of the form[1]

$$u_i^n=\xi^i(\Delta x)\tau^n(\Delta t), \tag{3}$$

the following CE emerges:

$$\tau+\tau^{-1}-2-\gamma^2(\xi+\xi^{-1}-2)=0. \tag{4}$$

Similarly, for the (2,4) difference equation

$$u_i^{n+1}+u_i^{n-1}+\left(\frac{5}{2}\gamma^2-2\right)u_i^n-\frac{4}{3}\gamma^2(u_{i+1}^n+u_{i-1}^n)+\frac{1}{12}\gamma^2(u_{i+2}^n+u_{i-2}^n)=0 \tag{5}$$

we have the following CE:

$$\tau+\tau^{-1}+\left(\frac{5}{2}\gamma^2-2\right)-\frac{4}{3}\gamma^2(\xi+\xi^{-1})+\frac{1}{12}\gamma^2(\xi^2+\xi^{-2})=0. \tag{6}$$

2.1.2. The two-dimensional wave equation

The two-dimensional case is also discretized via the second-order accurate, central difference (2,2) FDTD scheme as follows:

$$u_{i,j}^{n+1}-2u_{i,j}^n+u_{i,j}^{n-1}-\gamma_x^2\left[u_{i+1,j}^n-2u_{i,j}^n+u_{i-1,j}^n\right]-\gamma_y^2\left[u_{i,j+1}^n-2u_{i,j}^n+u_{i,j-1}^n\right]=0. \tag{7}$$

with $\gamma_x=\frac{c\Delta t}{\Delta x}$, $\gamma_y=\frac{c\Delta t}{\Delta y}$; $\Omega\triangleq\omega\Delta t$, $K_x\triangleq\beta_x\Delta x$, $K_y\triangleq\beta_y\Delta y$. Again, separating variables in the form of

$$u_{i,j}^n=\xi^i\eta^j\tau^n \tag{8}$$

one arrives at the following CE:

$$\tau+\tau^{-1}-2-\gamma_x^2(\xi+\xi^{-1}-2)-\gamma_y^2(\eta+\eta^{-1}-2)=0. \tag{9}$$

[1] This form is identical to the $\mathscr{Z}$-transform formulation.

2.2. The characteristic equation and dispersion relationship

2.2.1. The one-dimensional dispersion relationship

Once we define the eigenfunctions as $(\xi,\tau)=(e^{\jmath K},e^{\jmath\Omega})$ with $K\triangleq\beta\Delta x$ and $\Omega\triangleq\omega\Delta t$, the CE (4) translates into the familiar dispersion relationship for the (2,2) equation:

$$\sin^2\frac{\Omega}{2}=\gamma^2\sin^2\frac{K}{2}. \tag{10}$$

For the (2,4) equations, we again insert $\tau=e^{\jmath\Omega}$ $\xi=e^{\jmath K}$ into (6) to obtain the following dispersion relationship:

$$2\cos\Omega+\left(\frac{5}{2}\gamma^2-2\right)-\frac{4}{3}\gamma^2(2\cos K)+\frac{1}{12}\gamma^2(2\cos 2K)=0 \tag{11}$$

or

$$\gamma^2\sin^2\frac{K}{2}=\frac{1}{2}\left(\gamma^2-\left(4\pm\sqrt{9+\frac{12}{\gamma^2}\left(\sin^2\frac{\Omega}{2}\right)}\right)^2\right). \tag{12}$$

2.2.2. The two-dimensional dispersion relationship

In an analogous fashion to the 1D case, the dispersion relationship is produced by substituting the following into Eq. (9): $\xi=e^{\jmath K_x}\eta=e^{\jmath K_y}\tau=e^{\jmath\Omega}$ to obtain

$$\sin^2\frac{\Omega}{2}=\gamma_x^2\sin^2\frac{K_x}{2}+\gamma_y^2\sin^2\frac{K_y}{2}. \tag{13}$$

Eq. (13) tends to the nondispersive limit as Δt, Δx, $\Delta y\to 0$ or $\Omega\to 0$, i.e., Ω, K_x, $K_y\to 0$.

2.3. The characteristic equation and Von Neumann stability analysis

2.3.1. The one-dimensional stability criterion

Renaming $\tau=g$ in accordance with existing conventions, recalling $\xi=e^{\jmath K}$ and substituting into (4) for the (2,2) equations, the Von Neumann amplification polynomial is obtained:

$$g^2-2bg+1=0,\quad b=1+\gamma^2(\cos K-1). \tag{14}$$

$$\Rightarrow g_\pm=b\pm\sqrt{b^2-1}. \tag{15}$$

Eq. (2) is stable if $|g|\leqslant 1\Rightarrow b^2\leqslant 1$, i.e.

$$|1+\gamma^2(\cos K-1)|\leqslant 1\quad\forall K\Rightarrow\gamma^2\leqslant 1$$

which is the well-known Courant–Friedrich–Lövy condition.

For the (2,4) equations a similar procedure yields

$$\left|\frac{\left(\frac{5}{2}\gamma^2-2\right)-\frac{8}{3}\gamma^2\cos K+\frac{\gamma^2}{6}\cos 2K}{2}\right|\leqslant 1\quad\forall K \tag{16}$$

which, after some algebra, brings us to the well-known stability criterion $\gamma\leqslant\frac{\sqrt{3}}{2}$.

2.3.2. The two-dimensional stability criterion

Similarly to the 1D case, we rename $\tau=g$ and recall $\xi=e^{\jmath K_x}\eta=e^{\jmath K_y}$, such that Eq. (9) yields the 2D (2,2) FDTD Von Neumann amplification polynomial

$$g^2-2[1+\gamma_x^2(\cos K_x-1)+\gamma_y^2(\cos K_y-1)]g+1=0. \tag{17}$$

The stability criterion is then

$$|1+\gamma_x^2(\cos K_x-1)+\gamma_y^2(\cos K_y-1)|\leqslant 1 \quad \forall K_x,K_y \tag{18}$$

or, in its well-known form,

$$\gamma_x^2+\gamma_y^2\leqslant 1. \tag{19}$$

3. Methodology used for deriving reduced dispersion equations and stability criteria

A general process based on the use of the CE is now presented, incorporating schemes cited in Section 1 as special cases. It provides a methodology for formulating additional schemes that adhere to preset requirements relating to frequency coverage, phase or group velocity requirements, or control of directional properties in the nonisotropic grid. The process is outlined as follows:

1. Rearrange the characteristic equation in a standard form that includes the following terms:
   (a) Free coefficients that do not include τ or ξ.
   (b) Terms of the form $(\tau+\tau^{-1})$, $(\tau^2+\tau^{-2})$,... and $(\xi+\xi^{-1})$, $(\xi^2+\xi^{-2})$,... with appropriate coefficients.
   (c) In implicit cases, we also have terms of the form $(\tau\xi+\tau^{-1}\xi^{-1})$, $(\tau\xi^{-1}+\tau^{-1}\xi)$ with their respective coefficients.
2. Replace the aforementioned coefficients with a set of free parameters c_i, $i=1,2,\ldots$ to arrive at a *generalized characteristic equation*.
3. Choose a set of rules (e.g. elimination of phase or group velocity dispersion at designated frequencies or directions) to determine the c_is.
4. Replace the coefficients of the original difference equations with the c_is derived in step 3 thereby constructing the modified dispersion free difference equation.
5. Using the generalized characteristic equation, one can perform the Von Neumann stability analysis by substituting $\tau=g$ and recalling $\xi=\mathrm{e}^{\jmath K}$ such that the range of the parameters c_i can be determined.

Many sets of rules (step 3), facilitating variants of the method, are possible. Some of these rules have been in existence in other forms. In the sequel, rules for the elimination of either phase or group velocity dispersion at a prescribed normalized frequency Ω_0 are set as $v_{\mathrm{ph}}^{-1}|_{\Omega\to\Omega_0}=\frac{K}{\Omega}|_{\Omega\to\Omega_0}=\frac{1}{\gamma}$ and $v_g^{-1}|_{\Omega\to\Omega_0}=\frac{\mathrm{d}K}{\mathrm{d}\Omega}|_{\Omega\to\Omega_0}=\frac{1}{\gamma}$, respectively.

4. One-dimensional reduced dispersion difference equations

4.1. Dual rule reduced dispersion (2,2) FDTD

The process of Section 3 is now demonstrated with two rules for the one dimensional case. In accordance with step 1, rewrite first the CE (4) as

$$\tau+\tau^{-1}-2(1-\gamma^2)-\gamma^2(\xi+\xi^{-1})=0. \tag{20}$$

Next (step 2), replace two coefficients in (20) by the free parameters $c_{1,2}$:

$$\tau+\tau^{-1}-c_1-c_2(\xi+\xi^{-1})=0. \tag{21}$$

According to step 3, these parameters are determined by a set of two rules. As an example, choose the following set: elimination of phase velocity dispersion at two prescribed normalized frequencies $\Omega_{1,2}=\omega_{1,2}\Delta t$:

$$T_m-c_1-c_2\Xi_m=0, \quad m=1,2, \tag{22}$$

defining $T_{1,2}=\tau_{1,2}+\tau_{1,2}^{-1}=2\cos\Omega_{1,2}$, $\Xi_{1,2}=\xi_{1,2}+\xi_{1,2}^{-1}=2\cos K_{1,2}$, with $\tau_{1,2}=\mathrm{e}^{\jmath\Omega_{1,2}}$, $\xi_{1,2}=\mathrm{e}^{\jmath K_{1,2}}$, $K_{1,2}=\beta_{1,2}\Delta x=\frac{\Omega_{1,2}}{\gamma}$ (condition for zero phase velocity dispersion at these two frequencies). Note that both $T_{1,2}$ and $\Xi_{1,2}$ are real. Upon solving (22) for c_i we have

$$c_1=\frac{T_2\Xi_1-T_1\Xi_2}{\Xi_1-\Xi_2}, \quad c_2=\frac{T_1-T_2}{\Xi_1-\Xi_2}. \tag{23}$$

Using these coefficients, Eq. (2) is modified (step 4) as

$$u_i^{n+1} + u_i^{n-1} - \frac{T_2\Xi_1 - T_1\Xi_2}{\Xi_1 - \Xi_2}u_i^n - \frac{T_1 - T_2}{\Xi_1 - \Xi_2}(u_{i+1}^n + u_{i-1}^n) = 0. \tag{24}$$

For the special case where DC is included, i.e., $\Omega_1 = 0$, $\Omega_2 = \Omega_0$, Eq. (24) is reduced to

$$u_i^{n+1} - 2u_i^n + u_i^{n-1} - \frac{\sin^2\frac{\Omega_0}{2}}{\sin^2\frac{\Omega_0}{2\gamma}}(u_{i+1}^n - 2u_i^n + u_{i-1}^n) = 0. \tag{25}$$

One can see that Eq. (25) converges to the original difference Eq. (2) for both dispersion free cases, (a) $\gamma \to 1$ and (b) $\Delta t \to 0$, i.e., $\Omega_0 \to 0$.

A single frequency optimization can be useful for narrow-band, high-Q systems, where the temporal response can be quite lengthy and hence susceptible to dispersion errors. Dual and triple frequency cases (Section 4.3) can accommodate higher bandwidths.

4.2. Stability analysis for the dual rule reduced dispersion discrete wave equation

Completing the process of Section 3 with step 5, using the CE (21) and following the rationale of Section 2.3, one can obtain the following amplification polynomial:

$$g^2 - 2bg + 1 = 0 \tag{26}$$

with $b = \frac{1}{2}(c_1 2 + c_2(2\cos K))$. Therefore, stability is achieved if

$$|c_1 + c_2(2\cos K)| \leqslant 2 \quad \forall K. \tag{27}$$

Examining (27) at the extrema $K = 0$, π, respectively, we have the following inequality:

$$|c_1 \pm 2c_2| \leqslant 2. \tag{28}$$

For the nonmodified case $c_1 = 2(1 - \gamma^2)$, $c_2 = \gamma^2$, this criterion reverts to the well-known C.F.L. condition $\gamma^2 \leqslant 1$.

For the case $\Omega_1 = 0, \Omega_2 = \Omega_0$, the latter criterion is reduced to $\frac{\sin^2\frac{\Omega_0}{2}}{\sin^2\frac{\Omega_0}{2\gamma}} \leqslant 1$.

4.3. Triple rule reduced dispersion (2, 4) difference equation

Following step 2 of Section 3 for this scheme, we replace the coefficients of (6) with the free parameters $c_{1,2,3}$ to arrive at the following generalized characteristic equation:

$$\tau + \tau^{-1} + 2c_1 + c_2(\xi + \xi^{-1}) + c_3(\xi^2 + \xi^{-2}) = 0. \tag{29}$$

We make two choices for sets of three rules (step 3 of Section 3): the first one requires the elimination of phase velocity dispersion at three prescribed normalized frequencies, $\Omega_m = \omega_m \Delta t$, $m = 1, 2, 3$. Eq. (29) is then translated into the following system of linear equations:

$$2c_1 + \Xi_m c_2 + \Xi_m^{(2)} c_3 = -T_m, \quad m = 1, 2, 3. \tag{30}$$

where $T_m = \tau_m + \tau_m^{-1} = 2\cos\Omega_m$, $\Xi_m = \xi_m + \xi_m^{-1} = 2\cos K_m$, $\Xi_m^{(2)} = \xi_m^2 + \xi_m^{-2} = 2\cos 2K_m$, $\tau_m = e^{\jmath\Omega_m}$, $\xi_m = e^{\jmath K_m}$ and $K_m = \beta_m \Delta x = \frac{\Omega_m}{\gamma}$ (condition for zero phase velocity dispersion at these three frequencies). Solving for c_i in (30) and implementing step 4 of Section 3 would yield the modified difference equation for the (2, 4) case.

The second choice for a set of rules is the elimination of both phase and group velocity dispersion at $\Omega = 0$, with a third rule requiring the elimination of phase velocity dispersion at a prescribed normalized frequency Ω_1. For phase velocity dispersion elimination, we use Eq. (29) with $\Omega \to 0$:

$$1 + c_1 + c_2 + c_3 = 0. \tag{31}$$

A second equation is obtained from elimination of group velocity dispersion, i.e., $\left.\frac{dK}{d\Omega}\right|_{\Omega\to 0} = \frac{1}{\gamma}$. Upon differentiating (29) with $\tau = e^{\jmath\Omega}$ and $\xi = e^{\jmath K}$ we have

$$\frac{\mathrm{d}K}{\mathrm{d}\Omega} = \frac{-\sin\Omega}{c_2\sin K + 2c_3\sin 2K}. \tag{32}$$

Taking the limit $\Omega \to 0$ (implying $K \to 0$) and setting the result to be $\frac{1}{\gamma}$,

$$\left.\frac{\mathrm{d}K}{\mathrm{d}\Omega}\right|_{\Omega\to 0} = \frac{-\gamma}{c_2 + 4c_3} = \frac{1}{\gamma} \to c_2 = -(\gamma^2 + 4c_3). \tag{33}$$

For the third rule, Eq. (29) is to be satisfied for $K_1 = \frac{\Omega_1}{\gamma}$. This leads to

$$\cos\Omega_1 + c_1 + c_2\cos\frac{\Omega_1}{\gamma} + c_3\cos\frac{2\Omega_1}{\gamma} = 0. \tag{34}$$

Combination with Eqs. (31) and (33) yields:

$$c_3 = \frac{\left(\cos\frac{\Omega_1}{\gamma} - 1\right)\gamma^2 - (\cos\Omega_1 - 1)}{\left(\cos\frac{2\Omega_1}{\gamma} - 1\right) - 4\left(\cos\frac{\Omega_1}{\gamma} - 1\right)} \tag{35}$$

with companion solutions for c_1 and c_2.

One can examine this result for the limiting case $\Omega_1 \to 0$, i.e., in the conventional FDTD limit. To this end, we make use of the following approximations:[2]

$$\cos\Omega_1 - 1 \approx -\frac{1}{2}\Omega_1^2, \quad \cos\frac{\Omega_1}{\gamma} - 1 \approx -\frac{1}{2}\left(\frac{\Omega_1}{\gamma}\right)^2 + \frac{1}{24}\left(\frac{\Omega_1}{\gamma}\right)^4, \quad \cos\frac{2\Omega_1}{\gamma} - 1 \approx \frac{1}{24}\left(\frac{2\Omega_1}{\gamma}\right)^4 - \frac{1}{2}\left(\frac{2\Omega_1}{\gamma}\right)^2.$$

Substituting these approximations into (35), we have

$$c_{3_{\Omega_1\to 0}} = \frac{1}{12}\gamma^2 = c_3(\text{original FDTD}) \tag{36}$$

as expected. Further algebra shows that indeed

$$c_{2_{\Omega_1\to 0}} = -\frac{4}{3}\gamma^2 = c_2(\text{original FDTD}) \quad \text{and} \quad c_{1_{\Omega_1\to 0}} = \frac{5}{2}\gamma^2 - 2 = c_1(\text{original FDTD}). \tag{37}$$

Note that since the stencil required by the modified schemes is identical to the standard (2, 4) stencil, therefore issues related to implementations of PEC/PMC boundary conditions are the same as in the standard case.

5. Two dimensional reduced dispersion (2, 2) FDTD

The process of Section 3 can also be demonstrated for the two dimensional (2, 2) case. Rearranging Eq. (9) in the standard form (see step 1),

$$\tau + \tau^{-1} + 2(\gamma_x^2 + \gamma_y^2 - 1) - \gamma_x^2(\xi + \xi^{-1}) - \gamma_y^2(\eta + \eta^{-1}) = 0 \tag{38}$$

and replacing the coefficients according to step 2 to arrive at the generalized characteristic equation

$$\tau + \tau^{-1} + 2c_1 + c_2(\xi + \xi^{-1}) + c_3(\eta + \eta^{-1}) = 0, \tag{39}$$

one then can set $\tau = \mathrm{e}^{\jmath\Omega}$, $\xi = \mathrm{e}^{\jmath K_x}$, $\eta = \mathrm{e}^{\jmath K_y}$ into (39) to derive the generalized dispersion relationship

$$\cos\Omega + c_1 + c_2\cos K_x + c_3\cos K_y = 0 \tag{40}$$

that can be also be cast in term of the spectral direction ϕ as follows:

$$\cos\Omega + c_1 + c_2\cos(K\cos\phi) + c_3\cos(K\sin\phi) = 0. \tag{41}$$

At this point, one faces a wide choice of possible rules (step 3) for determining $c_{1,2,3}$ over the frequency-directions space, some of which would be treated in the context of this paper. As a first step, however, consider

[2] Note the higher order approximation of $\cos\frac{\Omega_1}{\gamma} - 1$ relative to $\cos\Omega_1 - 1$.

candidate rules prescribing $K_m = \frac{\Omega_m}{\gamma}$ (elimination of phase velocity dispersion) at three somes of points in this space:

Rule I Elimination of phase velocity dispersion at the points (ϕ_1, Ω_1), (ϕ_2, Ω_2), (ϕ_3, Ω_3). This leads to the system of linear equations:

$$\cos\Omega_m + c_1 + c_2\cos(K_m\cos\phi_m) + c_3\cos(K_m\sin\phi_m) = 0, \quad m = 1,2,3. \tag{42}$$

Rule II Same as Rule I at the points (ϕ_0, Ω_1), (ϕ_0, Ω_2), (ϕ_0, Ω_3), leading to the system

$$\cos\Omega_m + c_1 + c_2\cos(K_m\cos\phi_0) + c_3\cos(K_m\sin\phi_0) = 0, \quad m = 1,2,3. \tag{43}$$

Rule III Same as Rule I at the points (ϕ_1, Ω_0), (ϕ_2, Ω_0), (ϕ_3, Ω_0), leading to the system

$$\cos\Omega_0 + c_1 + c_2\cos(K_0\cos\phi_m) + c_3\cos(K_0\sin\phi_m) = 0 \quad m = 1,2,3. \tag{44}$$

5.1. Outline of stability analysis

Stability analysis would be pursued according to step 5 in Section 3. Redefine $\tau = g$ and recall $\xi = e^{jK_x}$, $\eta = e^{jK_y}$ in (39) to obtain the amplification polynomial

$$g^2 + 2(c_1 + c_2\cos K_x + c_3\cos K_y)g + 1 = 0. \tag{45}$$

Then, the following inequality needs to be worked out with the appropriate c_is:

$$|c_1 + c_2\cos K_x + c_3\cos K_y| = |c_1 + c_2\cos(K\cos\phi) + c_3\cos(K\sin\phi)| \leqslant 1. \tag{46}$$

6. Comparison with existing methods

A number of dispersion reduction schemes, reported recently in the literature, can be viewed as special cases within the general process of Section 3. Examples:

6.1. Nonstandard finite difference (NSFDTD) scheme [25]

In this scheme, Δt and $\Delta x = \Delta y = \Delta s$ are replaced by $\frac{2}{\omega_0}\sin\left(\frac{\omega_0\Delta t}{2}\right)$ and $\frac{2}{k_0}\sin\left(\frac{k_0\Delta s}{2}\right)$, respectively, to arrive at the following dispersion relationship:

$$\sin^2\left(\frac{\omega\Delta t}{2}\right) = \frac{\sin^2\left(\frac{\omega_0\Delta t}{2}\right)}{\sin^2\left(\frac{k_0\Delta s}{2}\right)}\left[\sin^2\left(\frac{k\Delta s\cos\phi}{2}\right) + \sin^2\left(\frac{k\Delta s\sin\phi}{2}\right)\right] \tag{47}$$

that eliminates phase velocity dispersion at $\Omega = \omega\Delta t = \Omega_0$, $K = k\Delta s = K_0$, $\phi = 0$. In comparison, the following three rules in our process, applied to Eq. (41) also lead to (47). The rules require zero phase velocity dispersion (recall: i.e., $K = \frac{\Omega}{\gamma}$) at: (I) $\Omega = 0\ \forall\phi$, (II) $\Omega = \Omega_0$, $\phi = 0$ and (III) $\Omega = \Omega_0$, $\phi = \frac{\pi}{2}$.

6.2. Isotropy-improved nonstandard finite difference [30]

In this scheme, two degrees of freedom augment the NSFDTD, thereby modifying (47) as

$$\sin^2\left(\frac{\omega\Delta t}{2}\right) = \frac{\sin^2\left(\frac{\omega_0\Delta t}{2}\right)}{\sin^2\left(\frac{k_0\Delta s}{2}\right)}\left[\frac{1}{a^2}\sin^2\left(\frac{k\Delta s\cos\phi}{2}\right) + \frac{1}{b^2}\sin^2\left(\frac{k\Delta s\sin\phi}{2}\right)\right]. \tag{48}$$

This scheme can be viewed as the following special case of our methodology, with the transformation

$$c_1 = \frac{2\mathscr{C}}{a^2} + \frac{2\mathscr{C}}{b^2} - 2, \quad c_2 = -\frac{2\mathscr{C}}{a^2}, \quad c_3 = -\frac{2\mathscr{C}}{b^2}, \quad \mathscr{C} \triangleq \sin^2\frac{\omega_0\Delta t}{2}.$$

Minimization of the average phase velocity dispersion error over all directions, forming the basis for [30], can be seen as synonymous with the following three rules: (I) $\Omega = 0$, $\phi = 0$, (II) $\Omega = \Omega_0$, $\phi = 22.5^0$ and (III) $\Omega = \Omega_0$, $\phi = 67.5^0$.

7. Dispersion analysis

Dispersion characteristics are initially demonstrated for the second variant of the three-rule case of the (2,4) scheme, in Section 4.3 (i.e., elimination of both phase and group velocity errors at $\Omega = 0$, and elimination of phase velocity error at a prescribed normalized frequency Ω_1). This choice affects the frequency and Courant number ranges over which dispersion would be minimized. Numerical experiments suggest that wider ranges are attained with the choice $\Omega_1 = \Omega_1(i) = \gamma_i$, such that Ω_1 can become a function of the spatial variable i for inhomogeneous media (note that optimization over a range of γ along the line of [5], would allow for determination of a single Ω_1 for the entire range, however our spatial dependence provides additional flexibility). For step function type of boundary conditions, it is well known that the global order of accuracy can be reduced, unless the discontinuity coincides with a grid plane at least for the (2,2) Yee staggered scheme (see, for example [38]). This issue is relevant for all FDTD schemes, therefore it is expected that the treatment for the modified schemes will be along similar lines. At this point we focus on the dispersion issues with possible discontinuities at grid planes.

Behavior of the phase (K vs. Ω) and group ($\frac{dK}{d\Omega}$ vs. Ω) velocity errors is analyzed using the dispersion curves, shown in Figs. 1–3 for the Courant numbers $\gamma = 0.8$, 0.6 and 0.4, respectively. Also shown is the case $\gamma = 0.9$ that is unstable for the conventional (2,4) scheme. The three cases shown on the K vs. Ω charts 1(a), 2(a), 3(a) and 4(a) pertain to the linear-ideal case, the (2,4) and the modified (2,4) schemes, while the four cases on the remaining $\frac{dK}{d\Omega}$ vs. Ω graphs are the linear-ideal case, the standard (2,2) and (2,4) and the modified (2,4) schemes.

Fig. 1 shows dispersion characteristics for $\gamma = 0.8$. In the K vs. Ω chart 1(a), one can see that the (2,4) curve lies underneath the ideal one for most of the frequency range, showing a higher phase and group velocities

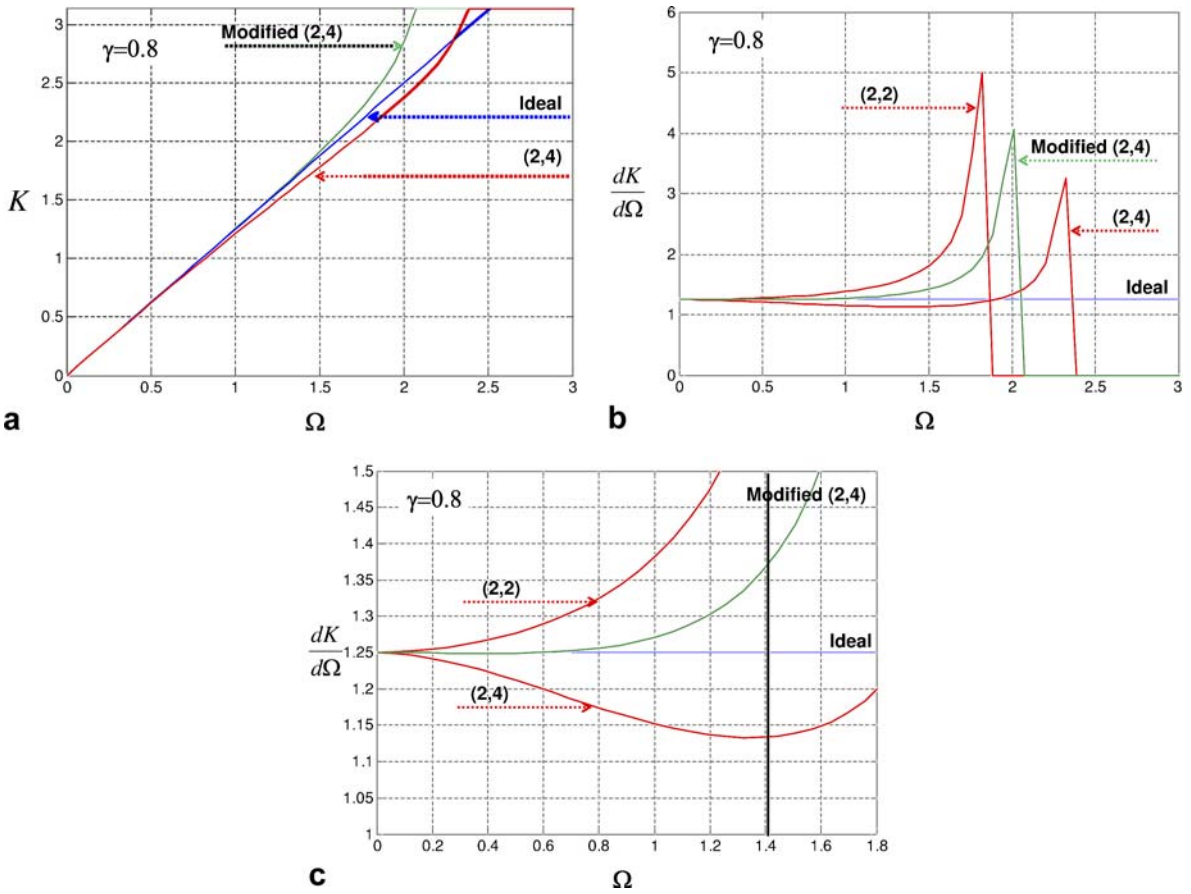

Fig. 1. Dispersion curves for the triple-rule modified (2,4) scheme, with $\Omega_1 = \gamma = 0.8$. (a) K vs. Ω, (b) $\frac{dK}{d\Omega}$ vs. Ω over the relevant frequency range, (c) blowup of (b) at the origin.

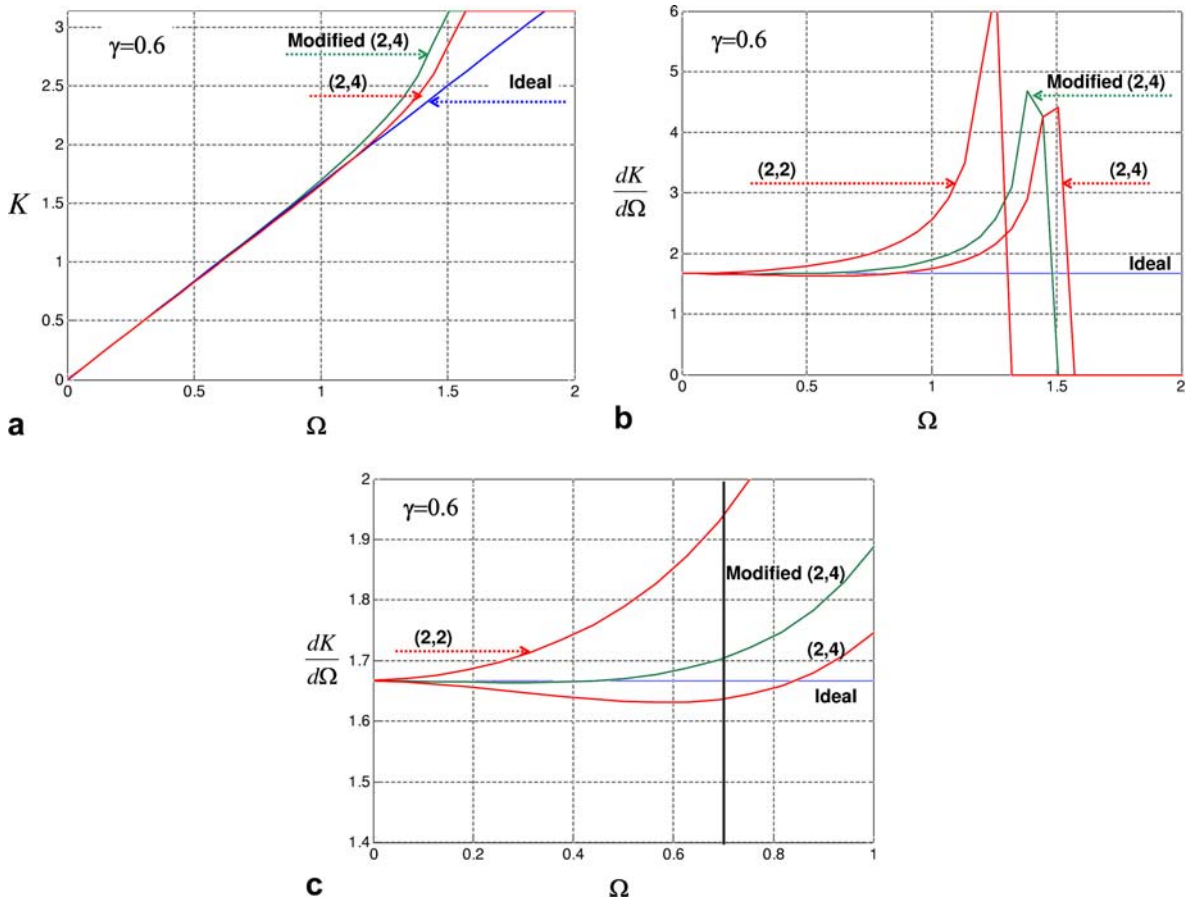

Fig. 2. Dispersion curves for the triple-rule modified (2,4) scheme, with $\Omega_1 = \gamma = 0.6$. (a) K vs. Ω, (b) $\frac{dK}{d\Omega}$ vs. Ω over the relevant frequency range, (c) blowup of (b) at the origin.

compared with the ideal case, typical of this scheme. This phenomenon, causing leading-edge distortion of pulses (as seen in the examples in Section 8), is indeed corrected by the modified (2,4) scheme, whose curve tracks the ideal one over a large part of the Ω scale. This benefit comes at the expense of a lower cutoff frequency, restricting somewhat the usage of the method to pulses within the narrower pass-band (termed "real numerical wavenumber regime" in [39]).

The derivatives of Fig. 1(a) are shown in Fig. 1(b). Any $\frac{dK}{d\Omega}$ vs. Ω graph (including Figs. 1(b), 2(b), 3(b) and 4(b)) can be divided into three regions, i.e., R1: a low- to mid-frequency region where the curve lies underneath the ideal curve, indicating the higher group velocity that translates to leading edge distortion as described above, R2: a high frequency area with a lower group velocity, causing trailing oscillations and R3: the cutoff region that leaves a small residual energy behind the pulse. Improvement in dispersion errors is expected over the first region of the standard (2,4) scheme.

As can be seen in Fig. 1(b), the modified (2,4) curve is aligned better with the ideal curve (that obeys the condition $\frac{dK}{d\Omega} = \frac{1}{\gamma}$) over R1, hence the improvement in dispersion errors over this region. Interestingly, the cutoff frequency of the modified (2,4) scheme is positioned between the corresponding frequencies of the (2,2) and (2,4) schemes, a phenomenon that stays consistent throughout the examples in the sequel. A closer inspection of the blown up Fig. 1(c) shows R1 with improved dispersion error, bounded by the break even (BE) point $\Omega_{BE} \approx 1.4$ as marked by the vertical solid line. This allows for analysis of fairly wideband pulses as demonstrated in Section 8. The behavior of the dispersion curve can be modified by more elaborate choices of Ω_1.

Fig. 2 shows similar dispersion curves for $\gamma = 0.6$. All cutoff frequencies decrease relative to the $\gamma = 0.8$ case. The BE point has now decreased to $\Omega_{BE} \approx 0.7$. The relative reduction in size of R1 will cause the corrective

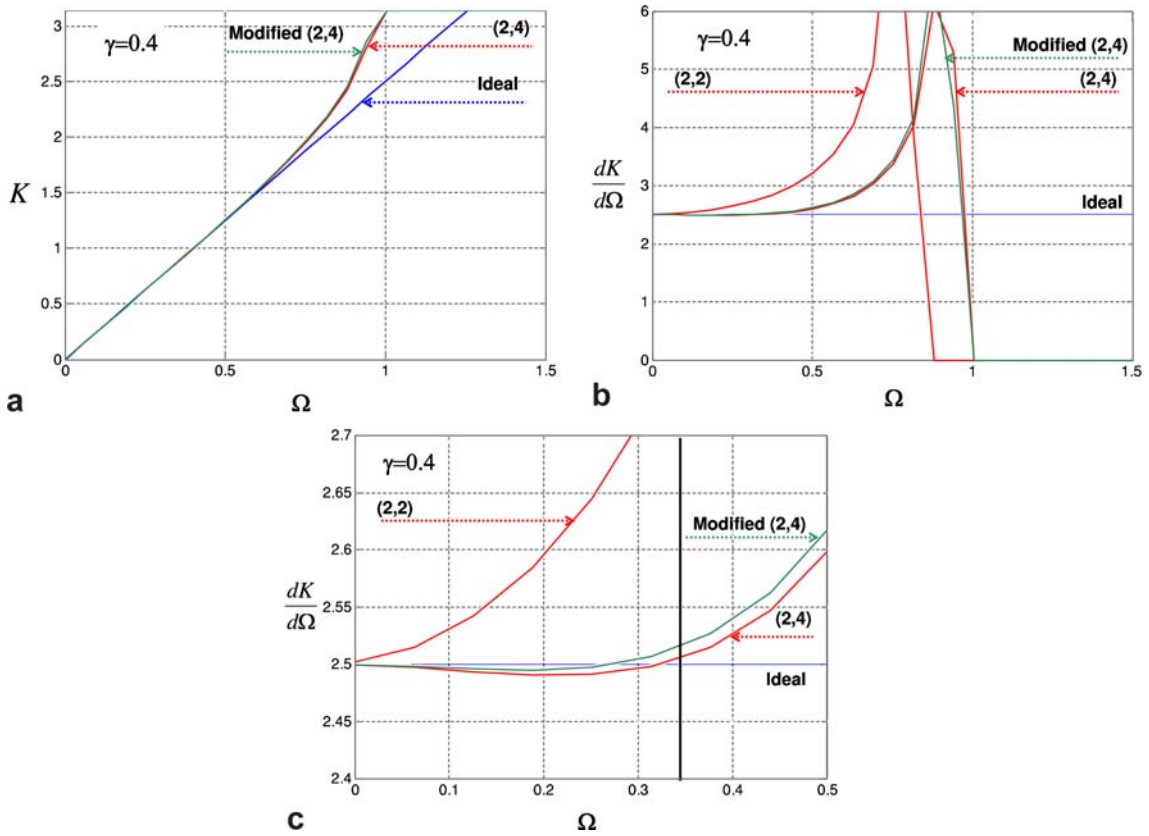

Fig. 3. Dispersion curves for the triple-rule modified (2,4) scheme, with $\Omega_1 = \gamma = 0.4$. (a) K vs. Ω, (b) $\frac{dK}{d\Omega}$ vs. Ω over the relevant frequency range, (c) blowup of (b) at the origin.

effect to be smaller. These trends continue into the $\gamma = 0.4$ case in Fig. 3, where the BE point is now at $\Omega_{BE} \approx 0.35$, showing a further reduction of R1 and hence a smaller expected corrective effect.

Reduction of dispersion errors will be stronger when the spectrum of the pulse is more thoroughly contained within the R1 region of the modified scheme. Because R1 increases with the value of γ, once can expect the modified scheme to perform better for higher values of γ. As the values of γ decrease, the spectrum may overflow into R3. In cases such as these, some effects of dispersion can be discerned from cutoff effects to show again the corrective effect of our scheme.

Fig. 4 relates to $\gamma = 0.9 > \sqrt{3}/2$, where the (2,4) scheme is unstable. It can be shown that the criterion for the modified (2,4) scheme is more relaxed, i.e., it is $\gamma \leqslant 1$. Therefore the modified scheme still operates beyond the stability limit of the regular (2,4) scheme.

8. Numerical results

For the sake of demonstration, we choose the following pulse shape

$$P(n) = \begin{cases} \sin^{\alpha}\left(\frac{\pi}{N}n\right), & 0 \leqslant n \leqslant N = 15 \\ 0, & \text{elsewhere} \end{cases} \qquad \alpha = 1, 2, 3,$$

as the excitation at $x = 0$ (see Fig. 5(a)). The pulse is sampled at the liberal rate of $M = 5$ samples per wavelength. The extent of the spectra in Fig. 5(b) can be compared with the sizes of R1 in Figs. 1–3 for the three values of γ in order to assess the effects mentioned in Section 7.

These effects are demonstrated in Figs. 6–8, that show snapshots and RMS errors of the pulse for $\alpha = 1$, 2 and 3, respectively. All snapshots are taken at $t = \tau\Delta t = \tau\gamma\frac{\lambda}{5c}$, where τ is the number of timesteps, such that

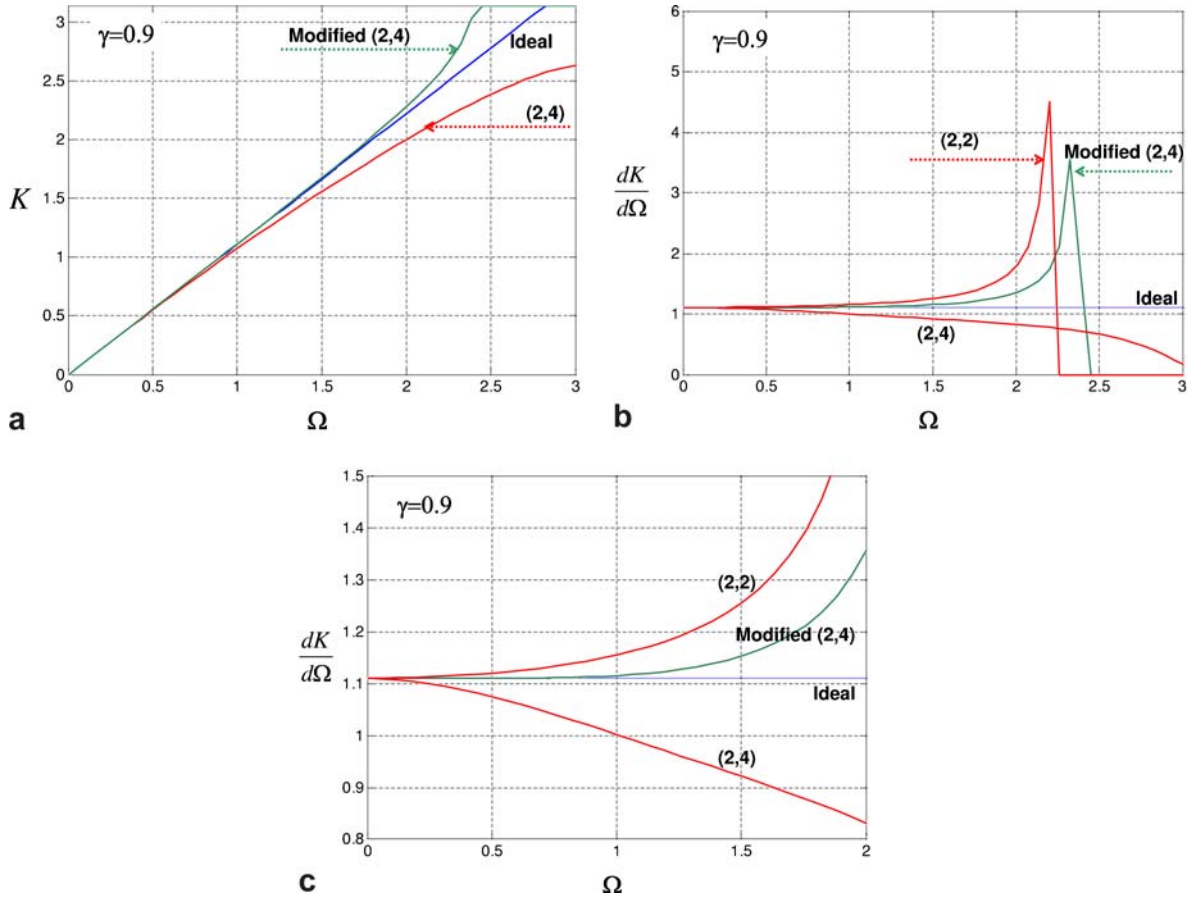

Fig. 4. Dispersion curves for the triple-rule modified (2,4) scheme, with $\Omega_1 = \gamma = 0.9$ (unstable (2,4) scheme). (a) K vs. Ω, (b) $\frac{dK}{d\Omega}$ vs. Ω over the relevant frequency range, (c) blowup of (b) at the origin.

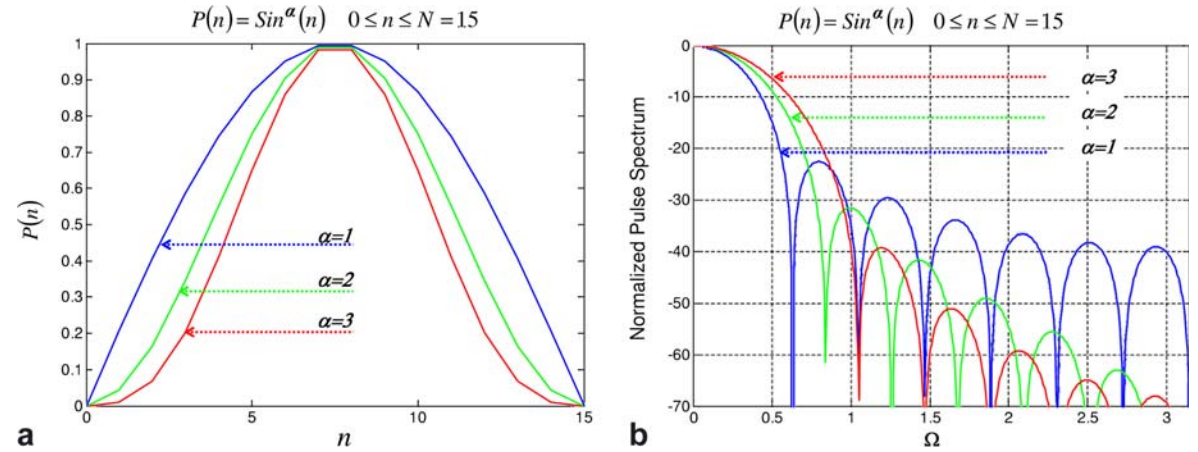

Fig. 5. $\sin^{\alpha}$ pulses, $\alpha = 1,2,3$. (a) Pulse shapes and (b) spectra vs. the normalized frequency $\Omega = \omega\Delta t$.

$t = \text{const.}$ for all values of γ. For $\gamma = 0.8$, the modified scheme yields a pulse that tracks the ideal one quite well in contrast to the pulse generated by the (2,4) scheme that is subject to severe dispersion errors due to the sparse sampling interval of $\frac{\Delta x}{\lambda} = 0.2$ (seen Figs. 6(a), 7(a) and 8(a)). In particular, leading edge distortions,

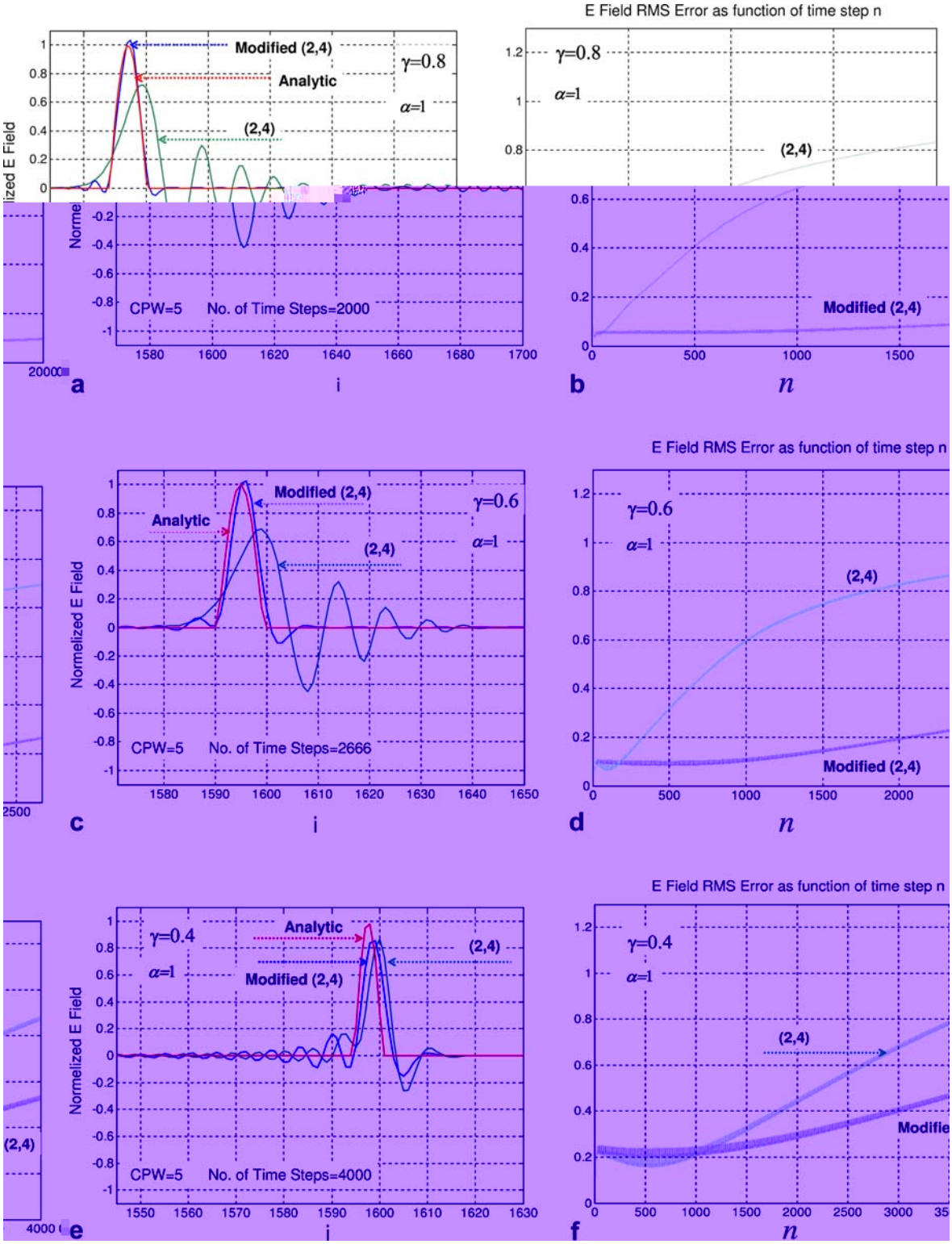

Fig. 6. Pulse propagation, $\alpha = 1$, $\Delta x = \frac{1}{5}$, $N = 15$. (a), (c), (e): snapshots at $\gamma = 0.8$, $\tau = 2000$; $\gamma = 0.6$, $\tau = 2666$; $\gamma = 0.4$, $\tau = 4000$. Exact solution, standard(2,4) FDTD scheme and three rule modified case. Leading edge distortion is corrected. (b), (d), (f): RMS errors, $\gamma = 0.8$, 0.6, 0.4.

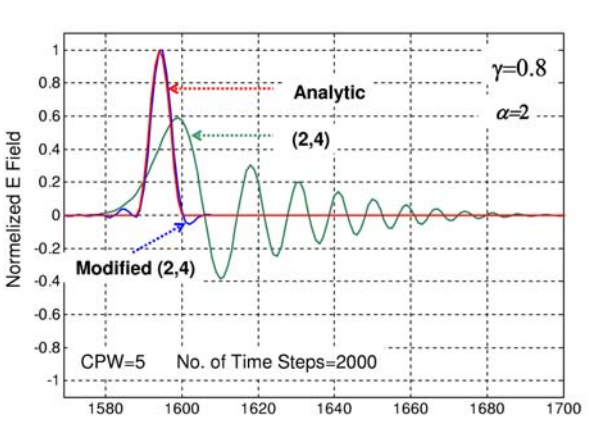

a

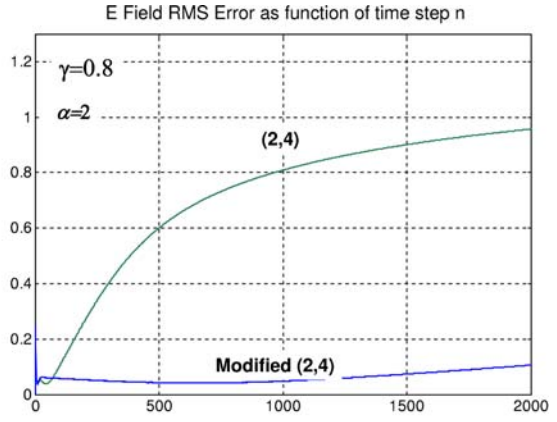

b

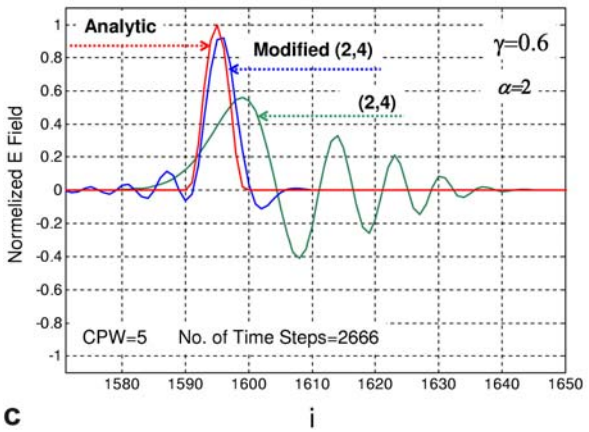

c

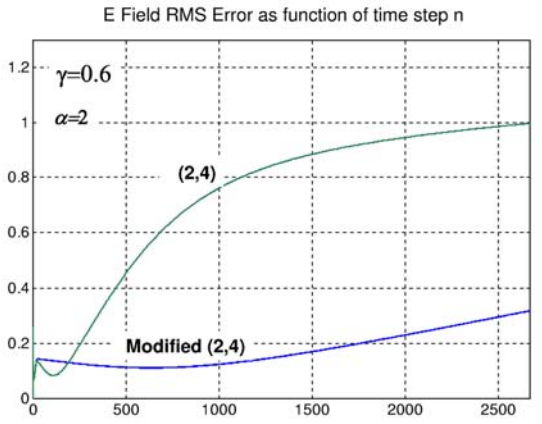

d

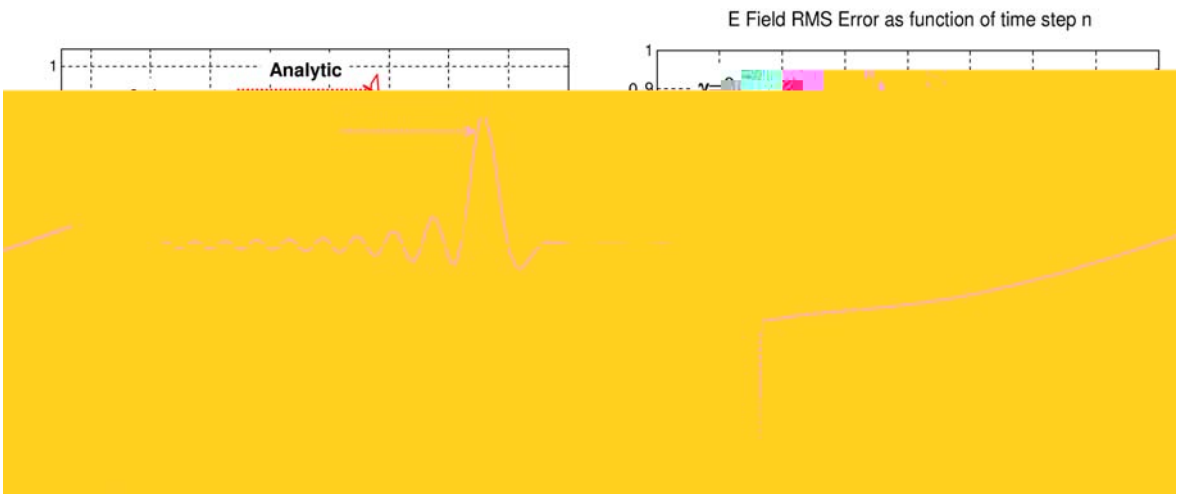

Fig. 7. Pulse propagation, $\alpha = 2$, $\Delta x = \frac{\lambda}{5}$, $N = 15$. (a), (c) and (e): snapshots at $\gamma = 0.8$, $\tau = 2000$; $\gamma = 0.6$, $\tau = 2666$; $\gamma = 0.4$ and $\tau = 4000$. Exact solution, standard (2,4) FDTD scheme and three rule modified case. Leading edge distortion is corrected. (b), (d) and (f): RMS errors, $\gamma = 0.8$, 0.6 and 0.4.

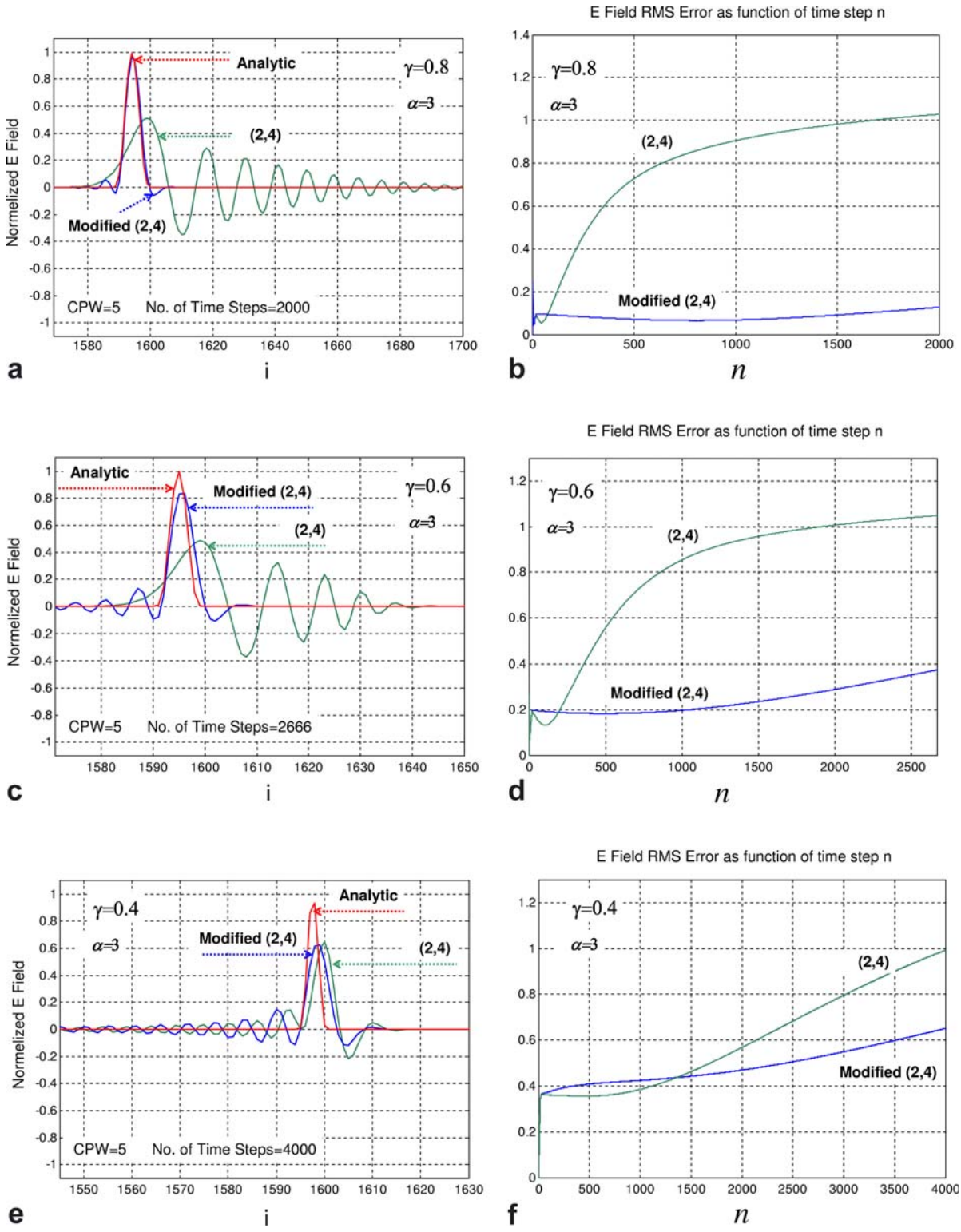

Fig. 8. Pulse propagation, $\alpha = 3$, $\Delta x = \frac{i}{5}$, $N = 15$. (a), (c) and (e): snapshots at $\gamma = 0.8$, $\tau = 2000$; $\gamma = 0.6$, $\tau = 2666$; $\gamma = 0.4$ and $\tau = 4000$. Exact solution, standard (2,4) FDTD scheme and three rule modified case. Leading edge distortion is corrected. (b), (d) and (f): RMS errors, $\gamma = 0.8$, 0.6 and 0.4.

resulting from the increase in group velocity discussed above, are quite significant for the (2,4) scheme. The modified scheme corrects this distortion as well as the group delay errors and the trailing ripples while sustaining the low sampling rate quite well. The resultant improvement is clearly visible in the RMS errors of the modified and original (2,4) schemes as they evolve over the entire temporal span $(0,t)$ in Figs. 6(b), 7(b) and 8(b). There errors are defined via integrations over the entire spatial domain, thus including all leading and trailing edge error sources.

Corresponding results for $\gamma = 0.6$ are seen in Figs. 6(c), 7(c) and 8(c), with RMS errors shown in Figs. 6(d), 7(d) and 8(d). A significant error reduction is seen for this value as well. For the case of $\gamma = 0.4$, (Figs. 6(e), 7(e) and 8(e)), The modified pulse is spread out and appears to be similar to the one obtained from the (2,4) scheme, however a careful analysis shows that a smaller group delay error is attained, its effect being manifested in reduced RMS error in Figs. 6(f), 7(f) and 8(f).

9. Conclusions

The strategy described in Section 3 provides a general framework for many existing as well as new schemes. The new schemes accommodate requirements for reduced phase or group velocity dispersion errors, defined over any region in the frequency-direction space, and used to determine the free parameters described above. The new and conventional schemes converge to the same continuous limit, while the new schmes maintain the same order of accuracy or better. Although the basic problem has been defined as a free space source problem, the effect of media with different parameters has been demonstrated. Von Neuman stability analysis has accompanied the development of the new schemes, helping determine the regions of applicability, that sometimes can exceed the original ones. Accuracy has been demonstrated both via dispersion curves and numerical examples that have included an RMS error criterion.

Further work on multidimensional cases, implicit operators and choice and implementation of absorbing boundary conditions (ABC) is under consideration for the next phase of this research.

References

[1] K.S. Yee, Numerical solution of initial boundary value problems involving Maxwell's equations in isotropic media, IEEE Trans. Antennas Propag. 14 (1966) 302.
[2] J. Fang, Time domain computation of Maxwell's equations, Ph.D. dissertation, University California at Berkeley, Berkeley, CA, 1989.
[3] K.L. Shlager, J.G. Maloney, S.L. Ray, A.F. Peterson, Relative accuracy of several finite-difference time-domain methods in two and three dimensions, IEEE Trans. Antennas Propag. 41 (1993) 1732.
[4] P.G. Petropoulos, Phase error control for FDTD methods of second and fourth order accuracy, IEEE Trans. Antennas Propag. 42 (1994) 859.
[5] Y. Liu, Fourier analysis of numerical algorithms for the Maxwell's equations, J. Comput. Phys. 124 (1996) 396.
[6] K. Lan, Y. Liu, W. Lin, A higher order (2,4) scheme for reducing dispersion in FDTD algorithm, IEEE Trans. Electromagn. Compat. 41 (1999) 160.
[7] A. Yefet, P.G. Petropoulos, A staggered fourth order accurate explicit finite difference scheme for the time domain Maxwell's equations, J. Comput. Phys. 168 (2001) 286.
[8] Z. Xie, C.H. Chan, B. Zhang, An explicit fourth order staggered finite difference time domain method for Maxwell's equations, J. Comput. Appl. Math. 147 (2002) 75.
[9] J.L. Young, D. Gaitonde, J.J.S. Shang, Toward the construction of fourth-order difference scheme for transient EM wave simulation:staggered grid approach, IEEE Trans. Antennas Propag. 45 (1997) 1573.
[10] E. Turkel, High order methods, in: A. Taflove (Ed.), Advances in Computational Electrodynamics – The Finite Difference Time Domain Method, Artech House, Norwood, 1998, pp. 63–110 (Chapter 2).
[11] J.S. Shang, High order compact schemes for time-dependent Maxwell's equations, J. Comput. Phys. 153 (1999) 312.
[12] E. Turkel, A. Yefet, On the construction of a high order difference scheme for complex domains in a Cartesian grid, Appl. Numer. Math. 33 (2000) 113.
[13] A. Yefet, E. Turkel, Fourth order compact implicit method for the Maxwell equations with discontinuous coefficients, Appl. Numer. Math. 33 (2000) 125.
[14] W.L. Miranker, Numer. Math. 17 (1971) 124.
[15] K.L. Lele, Compact finite difference schemes with spectral-like resolution, J. Comput. Phys. 103 (1992) 16.
[16] C.K.W. Tam, J.C. Webb, Dispersion-relation-preserving finite difference schemes for computational acoustics, J. Comput. Phys. 107 (1993) 262.
[17] Z. Haras, S. Ta'asan, Finite difference schemes for long-time integration, J. Comput. Phys. 114 (1994) 265.

[18] S. Wang, F.L. Teixeira, A three dimensional angle optimized finite difference time domain algorithm, IEEE Trans. Microw. Theory Tech. 51 (2003) 811.
[19] S. Wang, F.L. Teixeira, Dispersion-relation-preserving FDTD Algorithms for large-scale three-dimensional problems, IEEE Trans. Antennas Propag. 51 (2003) 1818.
[20] S. Wang, F.L. Teixeira, A finite difference time domain algorithm optimized for arbitrary propagation angles, IEEE Trans. Antennas Propag. 51 (2003) 2456.
[21] S. Wang, F.L. Teixeira, Grid dispersion error reduction for broadband FDTD electromagnetic simulations, IEEE Trans. Magn. 40 (2004) 1440.
[22] T.T. Zygiridis, T.D. Tsiboukis, Low dispersion algorithms based on higher order (2,4) FDTD method, IEEE Trans. Microw. Theory Tech. 52 (2004) 1321.
[23] G. Sun, C.W. Trueman, Optimized finite difference time domain methods based on the (2,4) stencil, IEEE Trans. Microw. Theory Tech. 53 (2005) 832.
[24] M. Popesu, W. Shyy, M. Garby, Finite volume treatment of dispersion relation preserving and optimized prefactored compact schemes for wave propagation, J. Comput. Phys. 210 (2005) 705.
[25] R.E. Mickens, Nonstandard Finite Difference Models of Differential Equations, World Scientific Publishing Company, Singapore, 1984.
[26] J.B. Cole, A high accuracy FDTD algorithm to solve microwave propagation and scattering problems on a coarse grid, IEEE Trans. Microw. Theory Tech. 43 (1995) 2053–2058.
[27] J.B. Cole, A high accuracy realization of the YEE algorithm using nonstandard finite differences, IEEE Trans. Microw. Theory Tech. 45 (1997) 991.
[28] J.B. Cole, High accuracy Yee algorithm based on nonstandard finite differences: new development and validations, IEEE Trans. Antennas Propag. 50 (2002) 1185.
[29] J.W. Nehrbass, J.O. Jevtić, R. Lee, Reducing the phase error for finite difference methods without increasing the order, IEEE Trans. Antennas Propag. 46 (1998) 1194.
[30] B. Yang, C.A. Balanis, An isotropy-improved nonstandard finite difference (2,2) scheme, in: Proceedings of the International IEEE/AP-S Symposium, Washington DC, July 2005.
[31] B. Yang, C.A. Balanis, High-order (2,4) standard finite difference scheme to improve anisotropy, in: Proceedings of the International IEEE/AP-S Symposium, Washington DC, July 2005.
[32] M.F. Hadi, M. Piket-May, A modified FDTD (2,4) scheme for modeling electrically large structure with high phase accuracy, IEEE Trans. Antennas Propag. 45 (1997) 254.
[33] E.A. Forgy, W.C. Chew, A time domain method with isotropic dispersion and increased stability on an overlapped lattice, IEEE Trans. Antennas Propag. 50 (2002) 983.
[34] Wagner, Schneider, J. Comp. Acoust. 13 (2005) 365.
[35] Z. Bi, K. Wu, C. Wu, J. Litva, A new finite difference time domain algorithm for solving Maxwell's equations, IEEE Micro Guided Wave Lett. 1 (1991) 382.
[36] M. Krumpholz, L.P.B. Katehi, MRTD: new time-domain schemes based on multiresolution analysis, IEEE Trans. Microw. Theory Tech. 44 (1996) 555.
[37] I. Tsukerman, Electromagnetic application of a new finite-difference calculus, IEEE Trans. Magn. 41 (2005) 2206.
[38] A. Ditkowski, K. Dridi, J.S. Hesthaven, Convergent cartesian grid methods for Maxwell's equations in complex geometries, J. Comput. Phys. 170 (2001) 39.
[39] A. Taflove, S.C. Hagness, Computational Electrodynamics – The Finite Difference Time Domain Method, 3rd ed., Artech House, Boston, 2005.